단축압출기내의 액적 변형과 파괴에 대한 연구

전한수, 황욱렬, 권태헌
포항공과대학교 기계공학과

Deformation Shape and Breakup of an Immiscible Drop in Single-Screw Extrusion Process

H.S. Jun, W.R. Hwang, T.H. Kwon
Department of Mechanical Engineering, Pohang University of Science & Technology.

Introduction

We investigated the deformation and the associated breakup of an immiscible drop in the single-screw extrusion process, by using the three-dimensional experimental flow-visualization techniques. A drop experiences continuously varying orientation and shear stress field, and this is why the classical drop deformation and breakup theories cannot be applied directly (see [1] for review of the classical theories and recent developments). However, the combination of existing theories presents a possible description method. Actually, the 2-zone model [2] roughly describes the breakup mechanism in the single-screw extruder. The sequence of alternating strong and weak zones well-suited for the helical deformation history of a particle in the process. Concurrently, Kang et al.[3] distinguished the cross-sectional regions into two subregions (inner and outer) according to the stress distribution on the particle path. In the inner region, they insisted that the classical Tomotika breakup mechanism (disintegration of thread at rest) dominate, whereas the tip-streaming breakup to occur in the outer region. But their works were restricted to the two-dimensional flow only, thus the effect of the longitudinal component and thereby the effect of the residence time distribution has been neglected. In this study, we present the 3-D experimental visualization results on drop deformation into a thread and its breakup of the two immiscible fluids with the comparable viscosity ratio $O(1)$, according to the spatial locations of the initial drop in the cross section.

Methods

The experimental apparatus is almost the same as that used in our previous study [4]. The flow in the single-screw extruder is modeled as a flow in the straight channel with an obliquely moving barrel plate on the top surface. The unwound channel is made of transparent acrylic plate and flipped upside down. The slider is located below the channel and is driven by an AC motor with the velocity control unit and a chain. To prevent leakages between the flight and the moving slider, rubber pads are located below the slider and are tightly fitted to both the slider and the channel. The height and the width of the channel are 4 cm and 8 cm, respectively (W/H = 2), to investigate the cross-sectional motion easily. The drag velocity of slider is adjusted to 9.72 cm/sec and the helix angle is 69 deg. to give more turns. The suspending matrix fluid is 1000 CS silicone oil (Shinetsu Silicone); and the drop fluid is a homogeneous mixture of Oil Blue N (Aldrich Chemical), 1-Bromonaphtalene, and Castor Oil (Aldrich Chemical). All of the above fluids and the fluid mixture are Newtonian. By changing the volume fraction of 1-Bromonaphtalene, the density of the drop can be controlled to obtain mutually buoyant mixture. The viscosities of the dispersed phase and the matrix phase are 0.70 Pa·sec and 0.976 Pa·sec, respectively. The corresponding viscosity ratio (λ) is determined as 0.7172. It is well known that it is easiest to deform and break the drop around $\lambda \sim 1$. The surface tension between the two fluids has been experimentally obtained according to Tomotika's linear theory [5] and the resulting value is σ=9.5 dyne/cm.

In the numerical part, we only consider the passive deformation in the numerical study, since the thread formation by the passive deformation is expected to affect largely on the breakup mechanism in our study. Velocity field is obtained by using the three-dimensional multi-variant finite element method and by assigning boundary conditions with the superposition principle [4]. We adjusted the value of the pressure gradient along the channel direction to give the same particle path in both the numerical tracking and the experiment. Numerical integration has been carried out by the fourth-order Runge-Kutta method. We also attempted to obtain the continuous three-dimensional passive deformations of an initial spherical drop with respect to time. During the numerical surface tracking, we inserted intermediate points implicitly so that a linear interpolated surface could generate the correct global configuration of the deformed drop.

An Example Result: Drop Deformation in Outer Region

A drop of 0.7 cm in diameter is placed at the 1 cm apart from the top no-slip surface (near the screw root). This region is characterized by the very high shear rate near the bottom surface (barrel surface) and the low shear rate near the top surface. The drop will experience the two different flow field periodically. Experimentally obtained continuous drop deformation and breakup results are indicated in Figure 2 (cross-sectional) and Figure 3 (longitudinal). Figures 2 and 3 indicate the experimental drop deformation and breakup results from CCD 1 and from CCD 2, respectively.

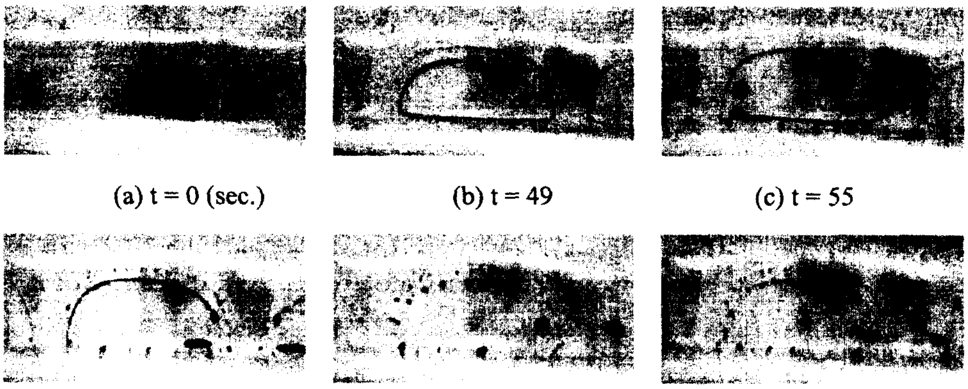

(a) t = 0 (sec.) (b) t = 49 (c) t = 55

(d) t = 63 (e) t = 74 (c) t = 100

Figure 2 Drop deformation and breakup in the outer region (cross-sectional).

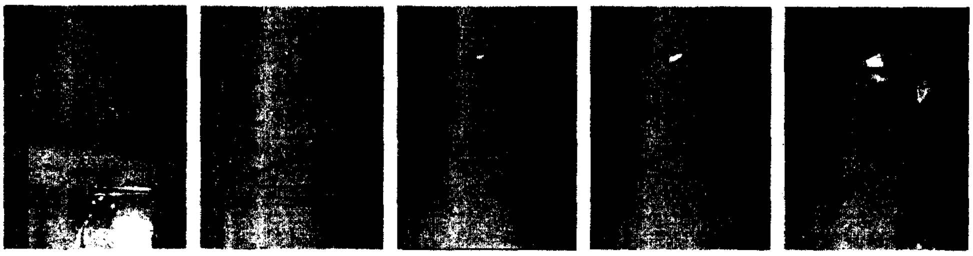

(a) t = 0 (sec.) (b) t = 39 (c) t = 52 (d) t = 56 (e) t = 72

Figure 3 Drop deformation and breakup in the outer region (longitudinal).

The initial configuration of the drop is a complete sphere (Figures 2a and 3a). However, as the drop flows along the flow field, it is continuously deformed to form a liquid thread (Figure 3b). An interesting point is the continuously varying cross-sectional radius in the thread from head to tail; bulbous head and decreasing cross-sectional radius to the tail. This phenomenon can be expected from the passive deformation patterns submerged in flows of the single-screw extrusion process. (Actually, the numerical passive deformation pattern of the drop shows good agreement with the experimental result in this case.) The reason would be two fold. One is the cross-sectional period distribution and the other is the residence-time distribution. The outer stream surface of the drop makes larger deformation than inner stream surface; and the inner orbit has smaller residence time so that it moves faster toward the outlet than the outer orbit. The breakup of the liquid thread is initiated from the bulbous head by the necking mechanism (see Figures 3b and 3c). But the next breakup starts from the tail end, where the radius of curvature is smallest, and then continuously propagates to the head along the thread. The breakups of the thread always occur when it enters the top surface (the entrance of the low shear region).

Conclusion

We investigated the deformation and the associated breakup of an immiscible drop in the single-screw extrusion process, by using the three-dimensional experimental flow-visualization technique. We realized the three-dimensional unwound channel flow with oblique drag that mimics the flow in the single-screw extrusion process. In experiments for the outer cross-sectional region, a drop is deformed into a comet-like liquid thread of large bulbous head and the long narrow tail with monotonically decreasing cross-sectional areas. This kind of deformation is due to the deformation characteristics of the single-screw extrusion process: the distributions of the cross-sectional period and residence time of the different stream surfaces on which the drop is located. The breakup of the liquid thread is initiated from the bulbous head by the necking mechanism. But the next breakup starts from the tail end, where the radius of curvature is smallest, and then continuously propagates to the head along the thread. The distribution of final drop sizes clearly shows monotonic decrease in size from head to tail. Opposed to this, the drop in the inner region does neither break into smaller drops nor form a liquid thread; instead, it experiences periodic ellipsoidal deformations.

References

1. Meijer, H.E.H. and Janssen, J.M.H, Mixing and Compounding: Theory and Practice, Manas-Zloczower, I. and Tadmor, Z., Eds., Hanser (1994).
2. Janssen, J.M.H and Meijer, H.E.H., *Polym. Eng. Sci.*, 35, 1766-1780 (1995).
3. Kang, J., Smith, T.G., and Bigio, D.I., *AIChE J.*, 42, 649-659 (1996).
4. Hwang, W.R., Jun, H.S., and Kwon, T.H., *AIChE J.*, submitted (2000).
5. Tomotika, S., *Proc. R. Soc. Lond. A*, 150, 322-337 (1935).